ELSEVIER

Biochimica et Biophysica Acta 1560 (2002) 25–36

BIOCHIMICA ET BIOPHYSICA ACTA
BBA

www.bba-direct.com

Interference of serum with lipoplex–cell interaction: modulation of intracellular processing

Inge S. Zuhorn [a], Willy H. Visser [a], Udo Bakowsky [a], Jan B.F.N. Engberts [b], Dick Hoekstra [a,*]

[a] *University of Groningen, Faculty of Medical Sciences, Department of Membrane Cell Biology, Bldg. 3215, 10th floor, A. Deusinglaan 1, 9713 AV Groningen, The Netherlands*

[b] *University of Groningen, Faculty of Chemistry, Department of Organic and Molecular Anorganic Chemistry, Nijenborgh 4, 9747 AG Groningen, The Netherlands*

Received 12 June 2001; received in revised form 21 November 2001; accepted 22 November 2001

Abstract

We have investigated the mechanism of lipoplex-mediated transfection, employing a dialkyl pyridinium surfactant (SAINT-2), and using serum as a modulator of complex stability and processing. Particle size and stability determine lipoplex internalization, the kinetics of intracellular processing, and transfection efficiency. Clustered SAINT-2 lipoplexes are obtained in the absence of serum (−FBS lipoplexes), but not in its presence (+FBS lipoplexes), or when serum was present *during* lipoplex formation [FBS], conditions that mimic potential penetration of serum proteins. The topology of DNA in [FBS] lipoplexes shifts from a supercoiled, as in −FBS lipoplexes, to a predominantly open-circular conformation, and is more prone to digestion by DNase. Consistently, atomic force microscopy revealed complexes with tubular extensions, reflecting DNA that protrudes from the lipoplex surface. Interestingly, the internalization of [FBS] lipoplexes is approximately three-fold higher than that of −FBS and +FBS lipoplexes, yet their transfection efficiency is approximately five-fold lower. Moreover, in contrast to −FBS and +FBS complexes, [FBS] complexes were rapidly processed into the late endosomal/lysosomal degradation pathway. Intriguingly, transfection by [FBS] complexes is greatly improved by osmotic rupture of endocytic compartments. Our data imply that constraints in size and morphology govern the complex' ability to interact with and perturb cellular membranes, required for gene release. By extrapolation, we propose that serum may regulate these parameters in an amphiphile-dependent manner, by complex 'penetration' and modulation of DNA conformation.

Keywords: Lipoplex; Transfection; Serum; Morphology; Intracellular processing; Cytoplasmic release

1. Introduction

The use of viral vectors for delivery of therapeutic genetic material into somatic cells (gene therapy) has several important drawbacks, including the risk of immunogenicity, potential recombination with endogenous viruses and cytotoxicity. Promising non-viral gene carriers are those that are based upon the use of cationic lipids. Because of their positive charge they spontaneously associate with negatively charged nucleic acids, thereby forming lipoplexes [1–3]. However, to match viral vectors, further improve-

* Corresponding author. Fax: +31-50-3632728.
E-mail address: d.hoekstra@med.rug.nl (D. Hoekstra).

0005-2736/02/$ – see front matter
PII: S0005-2736(01)00448-5

ment of their efficiency of delivery and gene expression is needed. This implies the need for further fundamental insight into the mechanism of amphiphile-mediated delivery, particularly in light of observations that the transfection efficiency of numerous cationic lipid formulations is reduced in the presence of serum. Specifically, a better understanding of lipoplex structure and stability is needed to clarify parameters that govern the mechanism of lipofection, thus providing tools for improving gene delivery.

Endocytosis is thought to represent a major entry pathway for productive transfection [4,5]. Szoka et al. [6] proposed a model for the destabilization of the complex and release of DNA into the cell's cytoplasm, a step which appears necessary for nuclear uptake and subsequent transcription of the exogenous DNA [4]. The involvement of endocytosis and lipoplex-mediated membrane destabilization in the transfection process necessarily imply that lipoplex size and stability, presumably dictated in part by the chemical nature of the amphiphile employed, should be important parameters in governing transfection efficiency, since the endocytic internalization capacity of cells, involving either coated or non-coated mechanisms, is restricted by particle size. Furthermore, once internalized, the complex should perturb the endosomal boundary and dissociate to allow the gene to acquire access to the nuclear transcription machinery.

In vitro, a reduced transfection efficiency is often been observed in the presence of serum [7–10]. In fact, serum may strongly interfere with lipoplex size, by preventing particle clustering, and affect particle stability. When assuming complex internalization to be required for cellular transfection, it would a priori be anticipated that smaller particles are more efficiently processed by cells and bring about transfection than larger complexes, which arise in the absence of serum. However, in spite of the enhanced size in the absence of serum, transfection at such conditions is often highly efficient, implying that factors other than size per se play a decisive role in determining efficiency. Indeed, it has been suggested that binding of serum proteins to the lipoplex prevents its interaction with the cell surface and/or its internalization, thereby inhibiting transfection [2,11,12]. However, no proportional correlation has been found between the cellular uptake of lipoplexes and their transfection efficiency [13,14]. Accordingly, given the need for intracellular release of plasmids as a crucial step in overall transfection, serum may also affect the stability of the particle [11,15], thus interfering with the cytosolic release and dissociation of the complex, following endocytic internalization [16]. However, little insight is available in these events at both the cellular and molecular level.

Recently, we synthesized a dialkyl pyridinium cationic amphiphile, SAINT-2, which efficiently transfects cells in vitro [17]. The size of the complex particles appears sensitive to serum, but the transfection efficiency is not [14,18]. In the present work we have examined the effect of serum on particle size and stability of SAINT/DOPE-DNA complexes, and examined the consequences in terms of lipoplex–cell interaction. The data lead us to propose that particle size and/or morphology govern the intracellular processing of lipoplexes in the endocytic pathway, (smaller) serum protein-'penetrated' particles being delivered to lysosomes prior to their ability to release their cargo from pre-lysosomal endocytic compartments. Transfection efficiency is thus determined by the stability of the complex, which can be regulated by the amphiphile-dependent nature of the interaction of serum proteins with such complexes.

2. Materials and methods

2.1. Preparation of liposomes and lipoplexes

A methanolic solution of SAINT-2, synthesized as described elsewhere [17], and DOPE (Avanti Polar Lipids, Alabaster, AL, USA) (1:1) was dried under a stream of nitrogen. The residual solvent was removed under vacuum. The lipid film was dissolved in Millipore water (lipid concentration: 1 mM) and sonicated to clarity in a bath sonicator. Liposomes (170 nm) and pDNA (pEGFP-N1, Clontech, Palo Alto, CA, USA) were taken up in equal volumes (0.5 ml) of serum-free cell culture medium and immediately mixed in a 2.5:1 molar charge ratio (15 nmol lipid; 1 μg DNA) by rapidly pipetting DNA to the liposome suspension. Lipoplexes (−FBS) were allowed to form for 10 min at room temperature before addition of serum in the case of transfection in the presence of serum (+FBS). Subsequently, lipo-

plexes were added to the cell culture. Alternatively, lipoplexes were also prepared in the presence of 10% serum, using serum-containing cell culture medium and following the same procedure as mentioned above. These particles are defined as [FBS] lipoplexes.

To examine the cellular fate of the complex by fluorescence microscopy, rhodamine-labeled lipoplexes were made by adding 0.5 mol% *N*-rhodamine-PE (Avanti Polar Lipids) to the initial SAINT-2/DOPE (1:1) solution. To examine the cellular association of lipoplexes radioactively labeled SAINT-2 was synthesized. For this purpose, the ammonium head group of the pyridine compound was quaternized using ^{14}C-labeled methyl iodide (Amersham, Amersham, UK).

2.2. Atomic force microscopy of lipoplexes

−FBS, +FBS, and [FBS] lipoplexes were prepared as described and after 1 h they were directly transferred onto a silicon chip by dipping the chip into the lipoplex solution. Atomic force microscopy was performed on a Digital Nanoscope IIIa Dimension 5000 (Digital Instruments, Santa Barbara, CA, USA) as described elsewhere [19]. The microscope was vibration-damped. Commercial pyramidal Si_3N_4 tips (NCH-W, Digital Instruments) on a cantilever with a length of 125 μm were used. The resonance frequency was about 220 kHz, and the nominal force constant was 36 N/m. All measurements were performed in Tapping mode to prevent damage of the sample surface. The scan speed was proportional to the scan size and the scan frequency was between 0.5 and 1.5 Hz. Images were obtained by displaying the amplitude signal of the cantilever in the trace direction, and the height signal in the retrace direction, both signals being simultaneously recorded. The results were visualized either in height or in amplitude modus.

2.3. Dextran density gradient of lipoplexes

Discontinuous dextran gradients were prepared as described by Eastman et al. [20], with some slight modifications. In brief, a stock solution of 30% (w/v) dextran T-500 (Amersham Pharmacia Biotech AB, Sweden), containing 5 μg/ml ethidium bromide (EtBr) was made in HBSS (Gibco, The Netherlands). Dilutions to 20%, 15%, 10% and 5% dextran were made with HBSS containing 5 μg/ml EtBr. 2 ml of each dextran dilution (30–5%) was layered in a centrifuge tube (Beckmann Ultraclear; 14×89 mm). Complexes, labeled with 5 mol% *N*-Rh-PE, were prepared in 1 ml HBSS and layered on top of the gradient. After addition of 1 ml HBSS containing 5 μg/ml EtBr, the gradients were centrifuged for 1 h (4°C) at 36 000 rpm. Photographs were taken using a Polaroid camera with normal light to visualize the lipids and UV light to visualize the DNA.

2.4. Agarose gel electrophoresis of lipoplexes

−FBS lipoplexes, +FBS lipoplexes, and [FBS] lipoplexes were suspended in HBSS (Gibco) and incubated for 10 min at 37°C, followed by treatment with DNase (1/2 h; 37°C) and/or Zwittergent (Calbiochem, San Diego, CA, USA), and loaded (in 30% glycerol) on a 0.8% agarose gel containing 1.25 μM EtBr. +FBS and [FBS] lipoplexes were treated with Zwittergent after proteinase K digestion (3.2 mg/ml). The latter was done to prevent the interaction of serum proteins with DNA after the release of DNA from the lipoplexes. Control experiments were carried out to verify the influence of the presence of serum proteins (10 and 50% FBS) as well as proteinase K on DNA conformation. Incubation of DNA with DNase for 1/2 h at 37°C resulted in a complete degradation of DNA (not shown). A current of 40 mA (80 V) was applied over the gel, immersed in 0.5 mM TBE buffer (0.045 M Tris–borate/0.001 M EDTA). The agarose gels were photographed with a Polaroid camera.

2.5. Transfection of COS-7 cells with SAINT-2/DOPE lipoplexes

1 day before transfection, COS-7 cells were plated in a 12-well plate (Costar, 1.3×10^5 cells/well). Prior to addition of the various lipoplexes, the cells were washed twice with HBSS (Gibco). Then 0.5 ml of the lipoplex mixtures, −FBS, +FBS or [FBS], prepared as described in Section 2.1 were added to the cells, and incubated at 37°C/5% CO_2. After 4 h the transfection medium was replaced by cell culture medium (DMEM; Gibco), containing 7% fetal bovine serum

(FBS), 2 mM L-glutamine (Gibco), 100 units/ml penicillin (Gist-Brocades, The Netherlands), 100 mg/ml streptomycin (Biochemie, Austria). After 24 h the cells were screened for reporter gene (green fluorescent protein) expression by FACS (Elite, Coulter; λ_{ex} 488 nm, λ_{em} 530 nm; 5000 events).

The cellular fate of the lipoplexes was examined by fluorescence microscopy (Olympus AX70 equipped with an Olympus PM-20 photography system).

For determination of the kinetics of lipoplex internalization by COS-7 cells, ^{14}C-labeled SAINT-2 was included in the lipid formulation. COS-7 cells were incubated with ^{14}C-labeled lipoplexes for 1–4 h. After the incubation, the cells were treated with CellScrub buffer (PBS-based buffer, composition proprietary; BIOzymTC BV, The Netherlands) to remove surface-bound lipoplexes (according to the manufacturer's procedure). The fraction of surface-bound and the fraction of internalized lipoplexes, defined as the fraction that was resistant to removal with CellScrub buffer, was counted on a scintillation counter. In a control experiment performed at 4°C (non-permissive temperature for endocytosis) it was determined that ~87% of the COS-7-associated SAINT/DOPE lipoplexes could be removed with CellScrub buffer. These data imply that less than 13% of the total cell-associated fraction remained adhered to the cells and/or the culture dish, following this treatment. Finally, in these experiments, cells and supernatants were separated by centrifugation (10 min at 800×*g*). At these conditions, pelleting of lipoplexes did not occur.

2.6. Osmotic rupture of endosomes during transfection of cells

After 1 and 4 h of incubation with lipoplexes, the cells were washed and subsequently subjected to an osmotic shock, using pinocytic cell loading reagent (Molecular Probes, Eugene, OR, USA), following essentially a procedure as provided by the manufacturer. Briefly, a hypertonic 1.5 M sucrose solution was added to the cells for 5 min at 37°C, followed by an incubation for 3 min with a hypotonic solution (cell culture medium diluted with deionized water (6:4 v/v)). These incubation times were optimized for the COS-7 cell line, implying that at the incubation conditions in these buffers significant cellular toxicity was not observed. The hypertonic sucrose solution will induce the formation of pinosomes that explode in the presence of the hypotonic buffer, releasing their content into the cell's cytoplasm. Cells were allowed to recover in cell culture medium for 1 day before transfection efficiency was determined by FACS analysis.

2.7. Lysosomal staining in COS-7 cells with LysoTracker Red

COS-7 cells were incubated with *N*-NBD-PE-labeled lipoplex for 1 h. Subsequently, cells were incubated for 15–30 min with 75 pM LysoTracker Red (Molecular Probes), washed and incubated for 30 min in normal medium to chase the LysoTracker Red into late endosomal/lysosomal compartments. Fluoromicrographs were taken with a confocal laser scanning microscope (Leica TCS SP2; Leica Microsystems, Germany), connected to a computer with Scanware software. Localization of lipoplexes in lysosomal compartments resulted in the colocalization of both fluorescent labels (green (lipid)+red (LysoTracker) = orange-yellow).

3. Results

3.1. Serum stabilizes the particle size of SAINT lipoplexes

To investigate the effects of particle size and stability on the interaction of lipoplexes with cells, we modulated these parameters by the presence of serum. By atomic force microscopy (Fig. 1) it was determined that SAINT-2/DOPE lipoplexes with a molar charge ratio of ~2.5 show an initial size distribution that varies between 200 and 400 nm. The round or oval-shaped lipoplexes have a smooth surface. However, upon incubation at room temperature, extensive aggregation occurs within a few hours, leading to clustered complexes with sizes that may exceed 1 μm (cf. Fig. 5). The addition of serum to preformed lipoplexes prevents this aggregation, thereby stabilizing the particle size of the lipoplexes. Interestingly, occasionally, we observed extensions on the surface of the lipoplexes, which extended towards an adjacent complex (Fig. 1b,

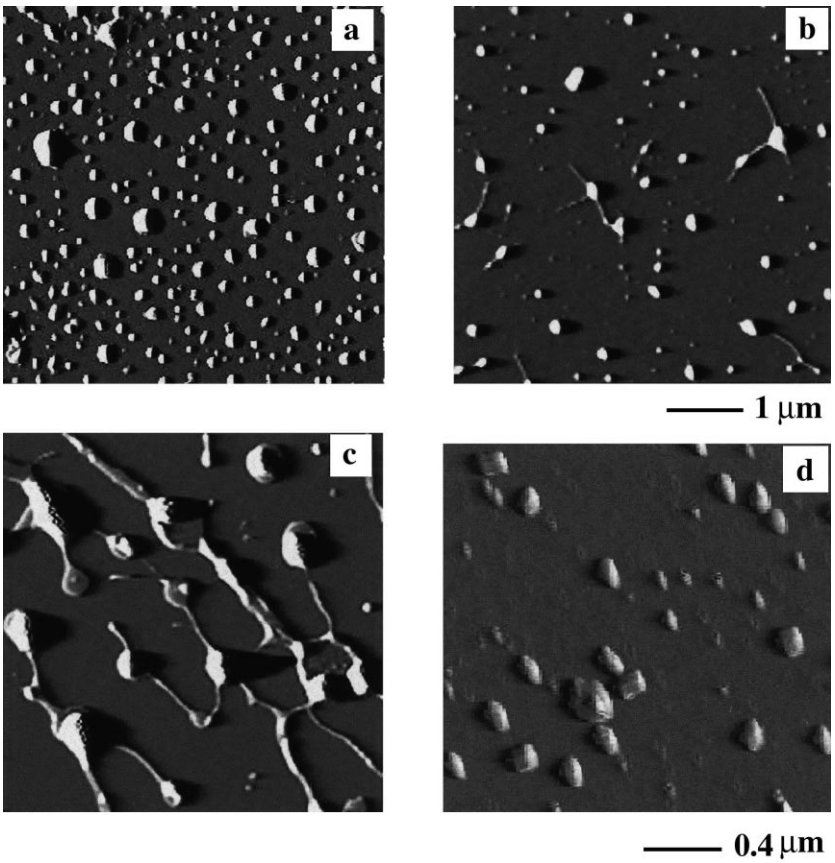

Fig. 1. Visualization of lipoplexes by atomic force microscopy (AFM). SAINT-2/DOPE (1:1) lipoplexes were prepared and examined by AFM as described in Section 2. (a) −FBS lipoplexes, visualized within 60 min after preparation. The lipoplexes display a smooth surface, while the size distribution varies between 200 and 400 nm. (b) +FBS lipoplexes were obtained by suspending −FBS complexes in serum-containing medium (10% FBS). After 60 min the sample was examined by AFM. Note the occasional presence of tubular extensions (upper right). (c) [FBS] lipoplexes were prepared by complex assembly in the presence of 10% FBS. After 30 min, the sample was examined by AFM. Note the extensive appearances of tubular structures extending from the complexes. The extensions originated from conformational changes of the DNA structure as treatment of (c) with DNase results in the appearance of complexes devoid of such extensions (d). Bar under (b) also applies to (a). Bar under (d) also applies to (c).

upper right corner). In principle, serum proteins may coat the complex or such proteins may, to various extents, penetrate into the complex, probably governed by the aggregate structure. To mimic such a condition, lipoplexes were also prepared in the presence of serum. These lipoplexes, assembled in serum ([FBS] lipoplexes), did not aggregate over the time intervals of the experiments and had a size distribution of 200–250 nm as determined by dynamic light scattering (data not shown). [FBS] lipoplexes showed similar tubular extensions, as observed upon exogenous addition of FBS following complex assembly, though much more abundant. To determine the stability of these complexes in terms of their size and ability of providing nucleic acid protection, we first performed a dextran density gradient centrifugation of the lipoplexes and investigated their nuclease accessibility.

3.2. *[FBS] lipoplexes show a decrease in size compared to −FBS and +FBS lipoplexes*

Dextran gradient centrifugation separates particles on the basis of size and density. Fig. 2 shows that SAINT-2/DOPE liposomes (I) appear as a distinct band in the 0% dextran layer. Free DNA (II) appears as a band on top of the 5% dextran layer with some diffuse label floating above the band. Note that for all the lipoplexes (III–V) the DNA label (EtBr) co-localizes with the lipid label (*N*-Rh-PE) (cf. Fig.

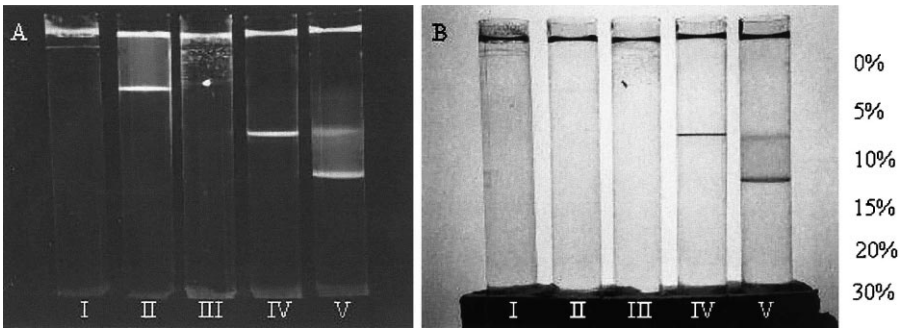

Fig. 2. Dextran density gradient of lipoplexes. Lipoplexes were prepared, treated with serum as indicated, and the lipoplex' size and density was determined by dextran density gradient centrifugation. I: SAINT-2/DOPE liposomes. II: Free DNA. III: −FBS lipoplexes. IV: +FBS lipoplexes. V: [FBS] lipoplexes. (A) UV-illuminated fluorescence micrograph, showing *N*-Rh-PE and EtBr (DNA) fluorescence. (B) Phase contrast picture showing *N*-Rh-PE. (The upper band that is present at the same level in each gradient is a reflection of the air–water interface (meniscus), an artifact of photography. Dextran gradient centrifugation of lipoplexes prepared in medium as compared to lipoplexes prepared in HBSS gives similar results.)

2A,B), implying that in all lipoplexes the DNA is complexed by lipids. −FBS lipoplexes (III) are floating on top of the gradient (0% dextran), like liposomes (I), but are heterogeneous in size. +FBS lipoplexes (IV) sediment on top of the 10% dextran layer as one distinct (homogeneous) band. Evidently, the addition of serum after complex formation (+FBS) prevents the aggregation (heterogeneous size distribution) of lipoplexes. In addition, the attachment of serum proteins might enhance the density of +FBS lipoplexes compared to −FBS lipoplexes, resulting in a sedimentation of +FBS lipoplexes further down into the gradient than in the case of −FBS lipoplexes. [FBS] lipoplexes equilibrate at an even higher density than −FBS and +FBS lipoplexes, i.e. they sediment at the top of the 15% dextran

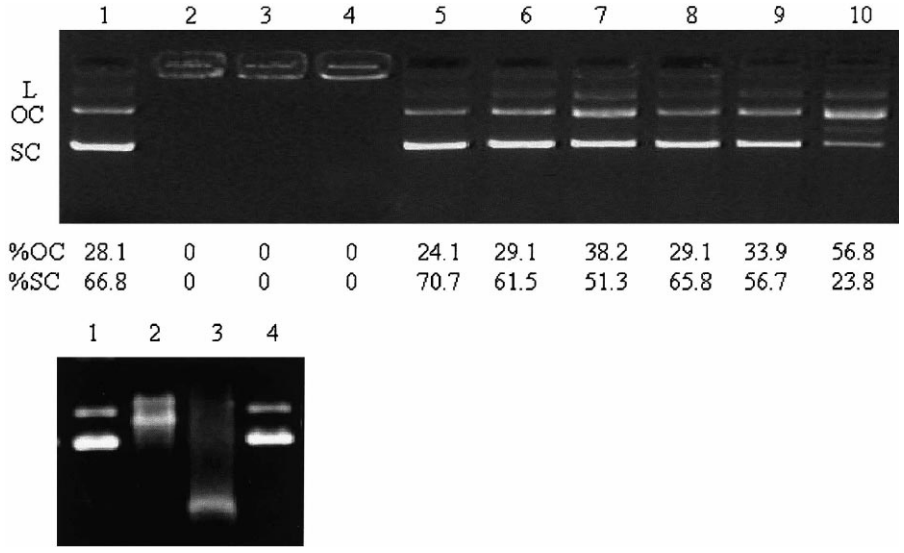

Fig. 3. Serum treatment of lipoplexes affects the DNA conformation and enhances nuclease accessibility. Lipoplexes were prepared, treated with serum as indicated, and the DNA conformation was analyzed by agarose gel electrophoresis, prior and after DNase treatment. Upper panel: Lane 1, 0.5 μg DNA (stock solution of pEGFP-N1). Lanes 2–4 contain untreated −FBS, +FBS, and [FBS] lipoplexes, respectively. Lanes 5–7 contain DNA released from lipoplexes (−FBS, +FBS, [FBS]), following treatment with Zwittergent. Lanes 8–10 show the DNA from lipoplexes (−FBS, +FBS, [FBS]), analyzed after their incubation with DNase (1/2 h, 37°C). The percentages of supercoiled (SC) and open-circular (OC) DNA in each sample are indicated. Lower panel: Lane 1, 0.5 μg DNA; lane 2, DNA treated with 10% FBS; lane 3, DNA treated with 50% FBS; lane 4, DNA treated with proteinase K, showing no influence of proteinase K on DNA conformation.

layer, with some lipoplexes remaining in the 10% dextran layer. The presence of serum during complex formation ([FBS]) apparently results in the assembly of lipoplexes that are smaller and/or more dense than −FBS and +FBS lipoplexes.

3.3. [FBS] lipoplexes show an enhanced nuclease accessibility compared to −FBS and +FBS lipoplexes

At a charge ratio of ∼2.5 no free DNA is present in the lipoplex formulation. As can be seen in Fig. 3, no migration of DNA into the agarose gel occurs. Incubation of lipoplexes in the presence of serum (+FBS) or preparation of lipoplexes in the presence of serum ([FBS]) neither resulted in migration of free DNA. This implies that the presence of serum does not prevent the association with or induces the dissociation of plasmid DNA from the cationic lipids (Fig. 3, upper panel, lanes 2–4). However, the presence of serum did affect the conformation of DNA in [FBS] lipoplexes. The DNA topology in these lipoplexes is shifted to an open-circular conformation compared to a predominantly supercoiled conformation in lipoplexes prepared in the absence of serum. This is visible after release of DNA from the lipoplexes by treatment with a detergent (Fig. 3, upper panel, lanes 5–7). In −FBS lipoplexes the DNA is completely protected from nuclease activity, while in both +FBS and [FBS] lipoplexes some of the DNA can be degraded by DNase treatment. After DNase treatment the conformation of DNA in [FBS] lipoplexes is largely open-circular while for −FBS and +FBS lipoplexes the major part of the DNA is still present in a supercoiled conformation. Apparently [FBS] lipoplexes show the highest nuclease accessibility, when compared to −FBS and +FBS lipoplexes (Fig. 3, upper panel, lanes 8–10). Interestingly, following treatment with DNase, atomic force microscopy measurements revealed that the tubular extension on the [FBS] complexes had essentially disappeared, and complexes could be seen with sizes varying between 200 and 300 nm (Fig. 1d).

3.4. Small-sized complexes are internalized by COS-7 cells to a higher extent than large complexes

An incubation of COS-7 cells with −FBS lipoplexes results in a similar amount of total cell association (surface-bound plus internalized) of lipoplexes as an incubation with +FBS lipoplexes. Interestingly, an almost two-fold increase in total cell association of [FBS] lipoplexes is obtained, compared to the other two types of lipoplexes. In fact,

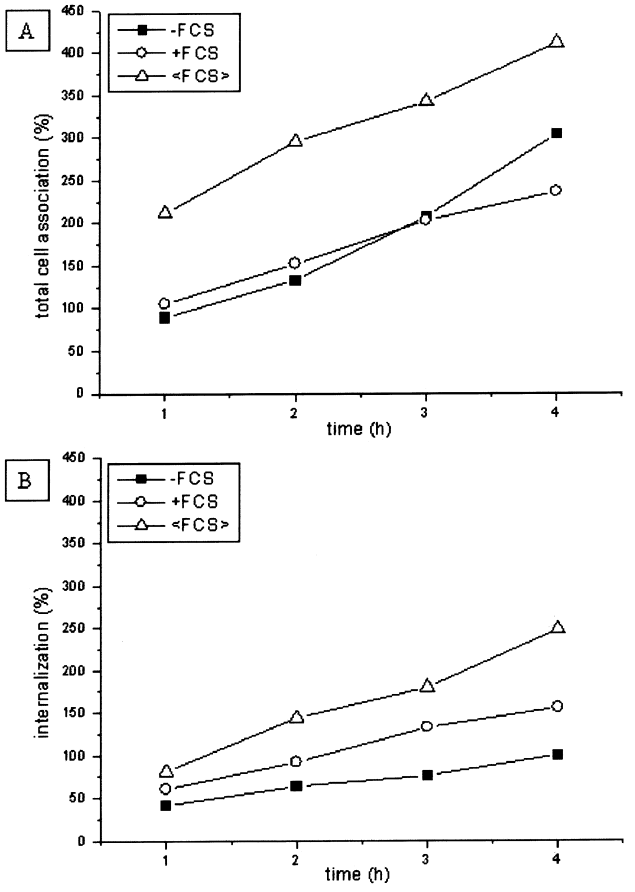

Fig. 4. Kinetics of total cell association and internalization of −FBS, +FBS and [FBS] lipoplexes by COS-7 cells. −FBS lipoplexes, +FBS lipoplexes and [FBS] lipoplexes, labeled with a trace amount of ^{14}C[SAINT-2], were incubated at 37°C with COS-7 cells as described in Section 2. After various time intervals, the cells were washed with HBS to remove loosely bound and non-cell-associated complexes. The cells were subsequently treated with CellScrub buffer (to remove tightly bound cell surface-associated complexes, see Section 2), trypsinized and centrifuged. The radioactivity of the supernatant and the cell pellet, representing surface-bound and internalized lipoplex respectively, was counted in a scintillation counter. The total cell-associated (radioactivity in supernatant and cell pellet) (a) and the internalized fraction (b) were plotted as a function of time. The data were expressed relative to those obtained for the internalization of −FBS lipoplexes. The internalization of −FBS lipoplex after 4 h of incubation was set as 100%. The experiment was performed twice in duplicate. S.D. ± 10%.

their internalization after 4 h of incubation is approximately three-fold higher than that of −FBS lipoplexes (Fig. 4).

As shown in Table 1, the presence of serum during transfection does not influence the transfection efficiency (i.e. in terms of number of cells transfected) of SAINT-2/DOPE lipoplexes. Indeed, −FBS and +FBS lipoplexes gave essentially the same transfection efficiencies of COS-7 cells. By contrast, transfection with [FBS] lipoplexes resulted in a 5–10-fold reduction in efficiency. Thus although the internalization of [FBS] lipoplexes is several-fold higher than that of −FBS lipoplexes, the transfection efficiency with these lipoplexes is almost an order of magnitude lower.

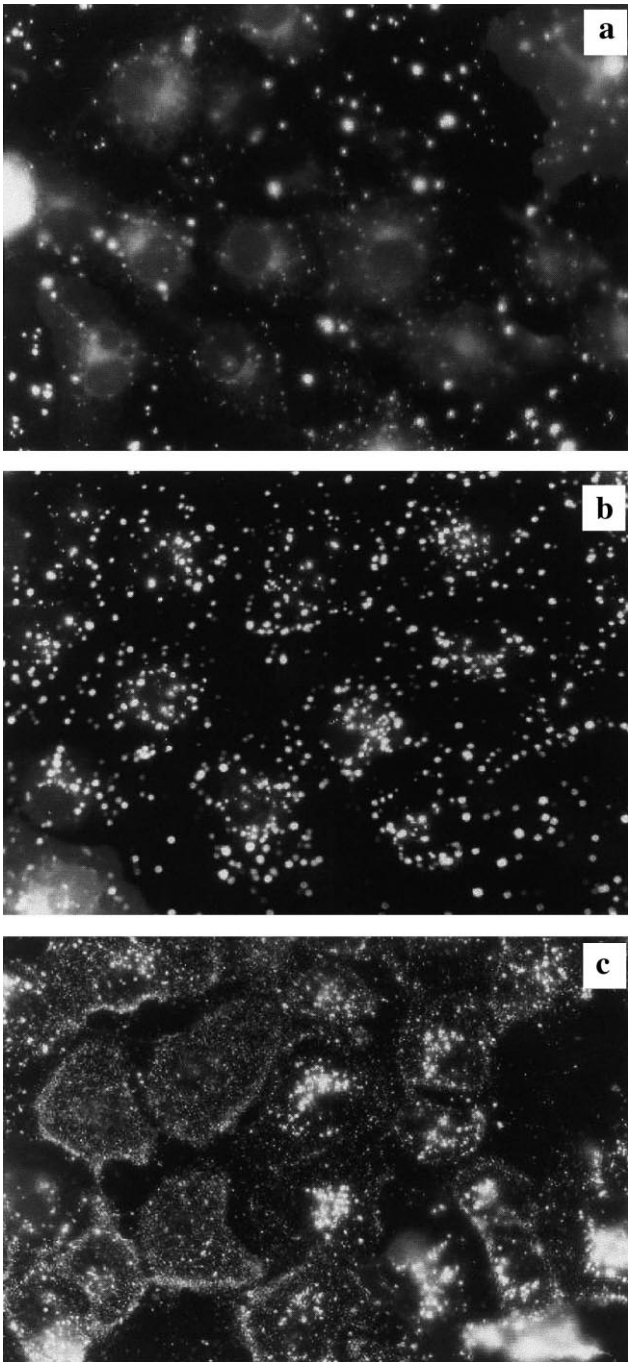

3.5. Rapid intracellular processing of [FBS] lipoplexes to lysosomes

Within 1 h after commencing transfection, [FBS] lipoplexes show a distinct perinuclear localization in COS-7 cells. By contrast, after 1 h −FBS and +FBS lipoplexes are distributed throughout the cytoplasm and at the cell periphery. Also note that in the absence of serum (−FBS), numerous large clustered particles are attached to the cells. In both cases, a pronounced perinuclear localization or accumulation is not observed (Fig. 5). Note that when we employed rhodamine-labeled plasmid (pGeneGrip, BIOzym, The Netherlands) as a lipoplex marker, instead of the lipid marker *N*-Rh-PE, indistinguishable fluorescence distribution patterns were observed (not shown). However, since the fluorescence resolution was less when applying the labeled plasmid, we carried out subsequent work with rhodamine-labeled lipid as a marker.

COS-7 cells that are incubated with *N*-NBD-PE-labeled [FBS] lipoplexes followed by loading with the lysosomal marker LysoTracker Red, show a perinu-

←

Fig. 5. Distribution of −FBS, +FBS and [FBS] lipoplexes in COS-7 cells, as revealed by fluorescence microscopy. COS-7 cells were incubated for 1 h (37°C) with lipoplexes, labeled with 0.5 mol% *N*-Rh-PE. Fluorescence microscopy was performed with an Olympus AX70 microscope equipped with an Olympus PM-20 photography system. Transfection with −FBS lipoplexes (a) results in a heterogeneous distribution of lipoplexes of different sizes, the largest complexes often associating with the cell periphery. Smaller complexes are found intracellularly, and diffuse fluorescence is often localized throughout the cytoplasm. Transfection with +FBS lipoplexes (b) results in a far more homogeneous distribution of lipoplexes that are equal in size, presumably localizing to endocytic compartments. COS-7 cells, incubated with [FBS] lipoplexes (c) are covered with small lipoplexes. Intracellularly, the [FBS] lipoplexes show a specific perinuclear localization.

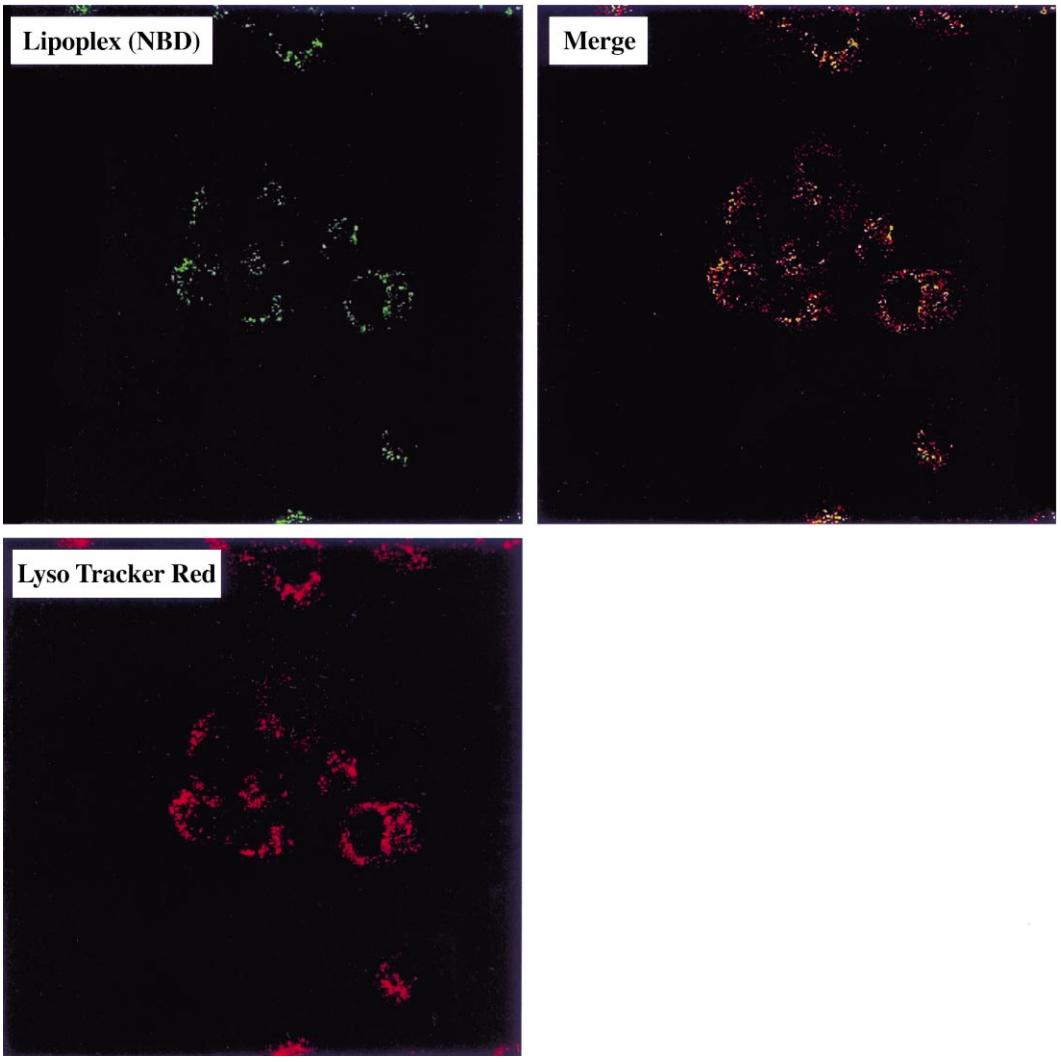

Fig. 6. Lysosomal localization of [FBS] lipoplexes. COS-7 cells were incubated for 1 h with *N*-NBD-PE-labeled (0.5 mol%) lipoplex (green) followed by a pulse-chase with LysoTracker Red, a lysosomal marker (Molecular Probes). With a confocal microscope two scans ($\lambda_{ex} = 488$ nm (green) and $\lambda_{ex} = 543$ nm (red)) were sequentially run in the plane of the nucleus. The images were merged using PaintShop Pro computer software. Incubation with [FBS] lipoplexes results in a colocalization (perinuclear) of lipoplex and the LysoTracker probe (yellow-orange in merged image). Thus [FBS] lipoplexes are located in late endosomes/lysosomes.

Table 1
Transfection efficiency with −FBS, +FBS, and [FBS] lipoplexes with and without an osmotic shock

Lipoplexes	Transfection efficiency ($t = 24$ h)	Transfection efficiency after osmotic shock ($t = 24$ h)	Multiplication factor
−FBS (1 h)	30.5 ± 3.5	36.2 ± 3.4	1.2
+FBS (1 h)	23.8 ± 1.0	42.4 ± 5.5	1.8
[FBS] (1 h)	2.3 ± 0.5	10.9 ± 2.6	5.3
−FBS (4 h)	50.9 ± 6.1	57.1 ± 3.5	1.1
+FBS (4 h)	50.2 ± 5.5	55.3 ± 5.5	1.1
[FBS] (4 h)	11.0 ± 4.9	17.5 ± 3.4	2.0

Values represent means of two experiments in duplicate, expressed as percentage of GFP-positive cells.

clear colocalization of the lysosomal marker and the lipoplexes (yellow-orange staining). Thus, these data indicate that the [FBS] lipoplexes are processed along the endocytic pathway, leading to their localization in late endosomal/lysosomal compartments (Fig. 6). When −FBS and +FBS lipoplexes were incubated over a similar time interval (1 h) with COS-7 cells, little if any overlap of both fluorophores was observed (cf. Fig. 5a,b versus Fig. 5c), implying that [FBS] complexes are more rapidly processed to a lysosomal destination than −FBS and +FBS complexes.

3.6. *Osmotic rupture of endosomes early during transfection enhances the transfection efficiency with [FBS] lipoplexes*

As shown above, the extent of internalization of lipoplexes by cells does not necessarily correlate with the transfection efficiency that is achieved with these lipoplexes. Thus in the presence of serum (+FBS and [FBS]) the internalization of complex was substantially higher than in the absence of serum, yet the transfection efficiency was the same or much less. Interestingly however, treatment of COS-7 cells with an osmotic shock after relatively short incubation times (1 h) significantly increased the transfection efficiency with +FBS and [FBS] lipoplexes, whereas a similar treatment of cells transfected with −FBS lipoplexes was substantially less effective (Table 1). For +FBS lipoplexes, the transfection efficiency almost doubled after osmotic shock, while transfection with [FBS] lipoplexes resulted in a more than five-fold increase in efficiency, increasing from less than 3% for the normal transfection procedure to 10–15% when, following a 1 h incubation, the cells were subjected to an osmotic shock. After 4 h of incubation, the shock procedure led to a less pronounced effect in all cases, although in an absolute sense a substantial increase up to about 20% transfection efficiency is reached in the case of [FBS] lipoplexes. Most likely, after 4 h of incubation a considerable amount of the internalized lipoplexes have reached compartments from which the release is less efficient after shock treatment than from compartments reached early after internalization (1 versus 4 h).

4. Discussion

The purpose of this work was to define the processing of lipoplexes by cells, using serum as a modulator of lipoplex size and stability, as serum–lipoplex interactions will have obvious implications for in vivo application. The data provide a rationale for the discrepancy between lipoplex internalization and transfection efficiency, the role of particle size/stability, and potential effects of serum on lipoplex processing and hence transfection efficiency.

In a previous study [14] we demonstrated that an incubation of lipoplexes prepared from either lipofectin or SAINT-2/DOPE in the presence of serum resulted in the binding of the same proteins to either complex. Yet, whereas lipofectin-mediated transfection was strongly inhibited in the presence of serum, little if any effect was observed when transfecting cells with SAINT complexes at the same conditions (cf. Table 1). Apparently, parameters other than simple steric interference of attached serum proteins with lipoplex–cell interaction determine the transfection capacity of a given complex. The present work strongly suggests that such interfering parameters may include the ability of serum proteins to penetrate into the complex, presumably determined by its structural integrity and 'internal' accessibility, which in turn is governed by the chemical nature of the amphiphile.

Clearly, neither the kinetics nor the extent of internalization represents a limiting step in overall transfection. On the contrary, both the cell association and the internalization of [FBS] lipoplexes is several-fold higher than that of either −FBS lipoplexes or +FBS lipoplexes. Rather, parameters following complex internalization appear to govern the effectiveness of subsequent transfection, in particular the timely release of the plasmid from the complex. The data (Table 1) indicate that this release is accomplished relatively early after internalization. Specifically, based upon the observations on the kinetics of processing of the [FBS] complexes and the strongly diminished transfection capacity of these complexes, the results imply that the more rapid the transport along the endocytic pathway, the slimmer the chances for productive transfection. Although upon extended incubation times of lipoplexes the size of

−FBS and +FBS may differ up to several-fold (between 1 μm and 200–400 nm, respectively), resulting in a less efficient internalization of −FBS complexes (Fig. 4B), there appears to be a balance between the rate of intracellular processing along the endocytic pathway and transfection efficiency, the latter being likely determined by the efficiency of cytosolic delivery of the plasmid. Apparently, arrival at the lysosomes precludes transfection (Fig. 5, Table 1), as occurs for [FBS] complexes, implying that factors that would delay lysosomal delivery and prolong the residence of lipoplexes in (early) endosomal compartments, will favor the efficiency of cellular transfection.

Escape from (early?) endosomal compartments will be determined by the efficiency of interaction of the complex with the endosomal membrane from within, and it is tempting to suggest that the dynamics of the amphiphile to perturb the (endosomal) bilayer structure will be instrumental in facilitating the plasmid's release. Such a membrane perturbing capacity of surfactants has been demonstrated before [21–23], and this feature may in part be related to their cytotoxic effects. In light of the present results it is relevant to note that when −FBS complexes (60 nmol total lipid/4 μg plasmid) were incubated with erythrocytes (10^8 cells), release of hemoglobin, as a measure of membrane perturbation, occurred, reaching a maximal release of approximately 30% after 15–20 min (not shown). By contrast, less than 5% release was observed in case of +FBS and [FBS] complexes, implying a reduced capacity of either complex to substantially perturb the target (erythrocyte) membrane structure. By extrapolation, these data would thus suggest that the serum-exposed complexes interact less efficiently with the endosomal membrane, resulting in a less efficient delivery of plasmid into the cytosol. Two pieces of evidence indicate however that during intracellular processing the lipoplexes may well undergo structural changes. First, +FBS complexes transfect cells as efficient as −FBS. This would suggest that the potential inhibitory effect of attached serum proteins on plasmid translocation must at least in part be relieved, when the complex resides in the endosomal compartment. Consistent with such a possibility is the observation that an osmotic shock, presumably lysing early endocytic compartments thereby allowing escape of lipoplexes into the cytosol, does result in a substantial enhancement of productive transfection, mediated by the serum-exposed complexes (Table 1). Although we cannot exclude that cytosolic compounds could also play a role in facilitating plasmid release, which is required for effective transcription [4,24], the fact that a much less pronounced increase occurs in case of −FBS complexes makes this possibility less likely. Thus, these data indicate that after internalization, the cytoplasmic delivery represents a significant barrier for efficient transfection, which appears to be affected by the relative ease of serum protein dissociation, determined by the amphiphile per se and lipoplex structure (e.g. SAINT-2/DOPE vs. lipofectin, see [14]).

When these proteins acquire subsequently access within the lipoplex structure, DNA conformational changes occur and protrusions extend on the complex surface, which further augment transfection inhibition, although the mechanism involved appears quite similar, i.e. interference with lipoplex–endosomal membrane interaction. Simulating such conditions by complex assembly in the presence of FBS, the results show that the DNA conformation in [FBS] lipoplexes has to a considerable extent been converted into an open-circular conformation, compared to a supercoiled structure in −FBS and +FBS lipoplexes (Fig. 3). Clearly, as a consequence, the packing is perturbed leading to surface protrusion of DNA (Fig. 1), as evidenced by their removal upon DNase treatment. It is conceivable that the tubular exposure of the nucleic acid will convey a negative charge to the lipoplex surface and a structural, steric hindrance for the cationic lipids to interact with the endosomal membrane. Given in addition their relatively small size, the particles are then rapidly reaching the lysosomes, as reflected by their perinuclear accumulation and colocalization with lysosomal markers (Fig. 6), representing the final destination in this degradation pathway.

Finally, since DNA in an open-circular conformation is transcriptionally less active than supercoiled DNA [25,26], this feature likely contributes in addition to the low transfection efficiency that is achieved with lipoplexes, whose structural properties allow serum penetration.

Taken together, we propose that structural parameters of the lipid formulation used for plasmid deliv-

ery are highly relevant towards the eventual outcome of transfection efficiency. When less tightly organized, proteins like those derived from serum could penetrate into the complexes, leading to DNA conformational changes and protein–amphiphile interactions that stabilize the membrane structure, thereby preventing an efficient early delivery of plasmids into the cytosol. Relatively small and stabilized particles may be rapidly processed along the endocytic pathway and become trapped into lysosomal compartments. Transfection appears to involve an escape from early compartments, and factors that prolong their localization in such compartments and favor efficient interactions between cationic lipid and endosomal membrane from within, promote transfection efficiency.

Acknowledgements

This work was supported by the Netherlands Foundation for Chemical Research (CW)/Netherlands Technology Foundation (STW) (349-4001). U.B. gratefully acknowledges support from the Leopoldina Foundation.

References

[1] O. Zelphati, F.C. Szoka Jr., J. Control. Release 41 (1996) 99–119.
[2] X. Gao, L. Huang, Gene Ther. 2 (1995) 710–722.
[3] P.L. Felgner, T.R. Gadek, M. Holm, R. Roman, H.W. Chan, M. Wenz, J.P. Northrop, G.M. Ringold, M. Danielsen, Proc. Natl. Acad. Sci. USA 84 (1987) 7413–7417.
[4] J. Zabner, A.J. Fasbender, T. Moninger, K.A. Poellinger, M.J. Welsh, J. Biol. Chem. 270 (1995) 18997–19007.
[5] A. El Ouahabi, M. Thiry, S. Schiffmann, R. Fuks, H. Ngyen-Tran, J.M. Ruysschaert, M. Vandenbranden, J. Histochem. Cytochem. 47 (1999) 1159–1166.
[6] Y. Xu, F.C. Szoka Jr., Biochemistry 35 (1996) 5616–5623.
[7] E.K. Wasan, P. Harvie, K. Edwards, G. Karlsson, M.B. Bally, Biochim. Biophys. Acta 1461 (1999) 27–46.
[8] V. Escriou, C. Ciolina, F. Lacroix, G. Byk, D. Scherman, P. Wils, Biochim. Biophys. Acta 1368 (1998) 276–288.
[9] L. Vitiello, K. Bockhold, P.B. Joshi, R.G. Worton, Gene Ther. 5 (1998) 1306–1313.
[10] J. Turek, C. Dubertret, G. Jaslin, K. Antonakis, D. Scherman, B. Pitard, J. Gene Med. 2 (2000) 32–40.
[11] O. Zelphati, L.S. Uyechi, L.G. Barron, F.C. Szoka Jr., Biochim. Biophys. Acta 1390 (1998) 119–133.
[12] J.G. Lewis, K.Y. Lin, A. Kothavale, W.M. Flanagan, M.D. Matteucci, R.B. DePrince, R.A. Mook Jr., R.W. Hendren, R.W. Wagner, Proc. Natl. Acad. Sci. USA 93 (1996) 3176–3181.
[13] A. Helbling-Leclerc, D. Scherman, P. Wils, Biochim. Biophys. Acta 1418 (1999) 165–175.
[14] S. Audouy, G. Molema, L. de Ley, D. Hoekstra, J. Gene Med. 2 (2000) 465–476.
[15] S. Li, F.C. MacLaughlin, J.G. Fewell, Y. Li, V. Mehta, M.F. French, J.L. Nordstrom, M. Coleman, N.S. Belagali, R.J. Schwartz, L.C. Smith, Gene Ther. 6 (1999) 585–594.
[16] P. Harvie, F.M.P. Wong, M.B. Bally, Biophys. J. 75 (1998) 1040–1051.
[17] A.A.P. Meekel, A. Wagenaar, J. Smisterova, J.E. Kroeze, P. Haadsma, B. Bosgraaf, M.C.A. Stuart, A. Brisson, M.H.J. Ruiters, D. Hoekstra, J.B.F.N. Engberts, Eur. J. Org. Chem. 3 (2000) 665–673.
[18] V. Oberle, I.S. Zuhorn, S. Audouy, U. Bakowsky, J. Smisterova, J.B.F.N. Engberts, D. Hoekstra, in: G. Gregoriadis, B. McCormack (Eds.), Targeting of Drugs: Strategies for Gene Constructs and Delivery, Nato Life Sciences, Amsterdam, 2000, pp. 146–155.
[19] V. Oberle, U. Bakowsky, I.S. Zuhorn, D. Hoekstra, Biophys. J. 79 (2000) 1447–1454.
[20] S.J. Eastman, C. Siegel, J. Tousignangt, A.E. Smith, S.H. Cheng, R.K. Scheule, Biochim. Biophys. Acta 1325 (1997) 41–62.
[21] H. Farhood, N. Serbina, L. Huang, Biochim. Biophys. Acta 1235 (1995) 289–295.
[22] I. Wrobel, D. Collins, Biochim. Biophys. Acta 1235 (1995) 296–304.
[23] I. van der Woude, A. Wagenaar, A.A. Meekel, M.B. ter Beest, M.H. Ruiters, J.B. Engberts, D. Hoekstra, Proc. Natl. Acad. Sci. USA 94 (1997) 1160–1165.
[24] O. Zelphati, F.C. Szoka Jr., Pharm. Res. 13 (1996) 1367–1372.
[25] C.R. Middaugh, R.K. Evans, D.L. Montgomery, D.R. Casimiro, J. Pharm. Sci. 87 (1998) 130–146.
[26] T.D. Xie, L. Sun, H.G. Zhao, J.A. Fuchs, T.Y. Tsong, Biophys. J. 63 (1992) 1026–1031.